Equilibrium and stability of dielectric elastomer membranes undergoing inhomogeneous deformation

Tianhu He [1,2], Xuanhe Zhao [2] and Zhigang Suo [2,a]

[1]*Key Laboratory of Mechanics on Western Disaster and Environment, and Department of Mechanics and Engineering Science, College of Civil Engineering and Mechanics, Lanzhou University, Lanzhou, Gansu 730000, PR China*

[2]*School of Engineering and Applied Sciences, Harvard University, Cambridge, MA 02138, USA*

Abstract

Dielectric elastomers are capable of large deformation subject to an electric voltage, and are promising for uses as actuators, sensors and generators. Because of large deformation, nonlinear equations of state, and diverse modes of failure, modeling the process of electromechanical transduction has been challenging. This paper studies a membrane of a dielectric elastomer deformed into an out-of-plane, axisymmetric shape, a configuration used in a family of commercial devices known as the Universal Muscle Actuators. The kinematics of deformation and charging, together with thermodynamics, lead to field equations that govern the state of equilibrium, as well as the conditions under which the state of equilibrium is stable. Numerical results indicate that the field in the membrane can be very inhomogeneous, and that the membrane is susceptible to several modes of failure, including electrical breakdown, electromechanical instability, loss of tension, and rupture by stretch. Care is needed in design to balance the requirements of averting various modes of failure while using the material efficiently.

Keywords: dielectric elastomer; large deformation; membrane; electromechanical instability

[a] email: suo@seas.harvard.edu

1. Introduction

As a class of materials for electromechanical transduction, dielectric elastomers posses a unique combination of attributes: large deformation, fast response, high efficiency, low cost, and light weight (Pelrine et al., 2000; Pelrine et al., 1998; Carpi et al., 2008). These attributes make dielectric elastomers promising for applications as transducers in, for example, cameras, robots, and energy harvesters (Bar-Cohen, 2002; Liu, et al., 2005; Wingert et al., 2006; Xia et al., 2005; Koford et al., 2007). The essential part of such a transducer is a membrane of a dielectric elastomer. Subject to a voltage, the membrane reduces its thickness and expands its area, converting electrical energy into mechanical energy.

To deform an elastomer appreciably, the electric field needed scales as $E \sim \sqrt{\mu/\varepsilon}$, where μ is the elastic modulus of the elastomer, and ε the permittivity. Using representative values, $\mu = 4\times10^{5}\,\mathrm{N/m^2}$ and $\varepsilon = 4\times10^{-11}\,\mathrm{F/m}$, one finds that actuating a dielectric elastomer requires an enormous electric field, on the order of $E \sim 10^{8}\,\mathrm{V/m}$. The intense electric field has major consequences in the design of transducers. The membrane nearly always operates on the verge of *electrical breakdown*, where the electric field may mobilize charged species in the elastomer to produce a path of electrical conduction. The membrane is also susceptible to an instability specific to deformable dielectrics. As the applied voltage is increased, the elastomer reduces thickness, so that the voltage induces an even higher electric field. The positive feedback between a thinner elastomer and a higher electric field may cause the elastomer to thin down drastically, resulting in *electromechanical instability* (Stark and Garton, 1955). Furthermore, to avoid excessively high voltage in use, the membrane must be thin. For example, an electric field of $10^{8}\,\mathrm{V/m}$ in a 1 mm thick membrane requires a voltage of $10^{5}\,\mathrm{V}$. The thin membrane, however, buckles under slight compressive stresses in its plane. Even for a pre-tensioned membrane, the applied voltage induces deformation, which may remove the tensile prestress, a condition known as *loss of tension*. Of course, when the polymer chains in the membrane are stretched severely, the membrane is susceptible to *rupture by stretch*.

While these modes of failure are known to limit the performance of dielectric elastomer transducers, few systematic studies have been reported (Plante and Dubowsky, 2006; Moscardo et al., 2008). Modeling dielectric elastomer transducers has been challenging due to the diverse modes of failure, as well as large deformation and nonlinear equations of state (Wissler and Mazza, 2005a, 2005b, 2007a, 2007b). This paper explores these issues by studying a membrane of a dielectric elastomer deformed into an out-of-plane, axisymmetric shape (Fig. 1), a configuration used in a family of commercial devices known as Universal Muscle Actuators (UMAs), marketed by Artificial Muscle, Inc. While many other configurations have been proposed in the literature, the focus on a particular configuration, such as the UMAs, may bring the benefits of standardization while still addressing a large range of early applications (Bonwit et al., 2006; Duncheon, 2008). To focus our attention even further, this paper will be restricted to the fundamental issues of electromechanics of membranes. In particular, attention here will be placed on a single membrane as illustrated in Fig. 1, rather than two membranes used in UMAs.

The study of axisymmetric deformation of membranes has a long tradition (e.g., Adkins and Rivlin, 1952; Tezduyar et al., 1987). Also studied recently is the axisymmetric deformation of membranes subject to electromechanical loads (Goulbourn et al., 2005; Mockensturm and Goulbourne, 2006; Goubourne et al., 2007). In this paper, we use these analytical and computational tools to study various modes of failure. We combine the kinematics of axisymmetric deformation of membranes and the thermodynamics of elastic dielectrics. This approach follows the recent studies of elastic dielectrics (McMeeking and Landis, 2005; Dorfmann and Ogden, 2005; Suo et al., 2008). Governing equations derived here recover those in Goulbourn et al. (2005) for an idealized material model, and can accommodate more general material models. We further derive the condition under which an inhomogeneous state of equilibrium is stable against inhomogeneous perturbation. We then describe numerical results for the specific configuration illustrated in Fig. 1. We show that the field in the membrane can

be highly inhomogeneous, such that a judicious design is needed to avert various modes of failure, while using the material efficiently.

2. State of equilibrium

Fig. 1 illustrates the cross section of a membrane of a dielectric elastomer. A circular dielectric membrane is coated on both surfaces with compliant electrodes. In the undeformed state (Fig. 1a), the membrane is of thickness *H* and radius *B*. A specific particle of the membrane is at a distance *A* from the center O, and a general particle is at a distance *R* from the center. In the deformed state (Fig. 1b), the membrane is attached to a rigid disk of radius *a*, and to a rigid ring of radius b, such that the particle *A* moves to the place *a*, and the particle *B* moves to the place *b*. When a force *F* is applied to the disk and a voltage Φ is applied between the two electrodes, the disk moves relative to the ring by a distance *u*, and an amount of charge *Q* flows from one electrode to the other. Meanwhile the membrane deforms into an out-of-plane, axisymmetric shape.

Following Adkins and Rivlin (1952), we first examine the kinematics of deformation. In the deformed state (Fig. 1b), the particle *R* moves to a place with coordinates *r* and *z*. The two functions, $r(R)$ and $z(R)$, fully describe the deformed shape, and are subject to the following boundary conditions: $r(A)=a$, $r(B)=b$, $z(A)=u$ and $z(B)=0$. Consider the longitudinal stretch by examining two nearby particles, R and $R+dR$. In the deformed state, the two particles occupy places separated by $dr=r(R+dR)-r(R)$ and $dz=z(R+dR)-z(R)$. Let dl be the distance between the two particles when the membrane is in the deformed state, and $\theta(R)$ be the slope of the vector connecting the two particles, so that $dr=\cos\theta dl$, $dz=-\sin\theta dl$, and $(dl)^2=(dr)^2+(dz)^2$. The longitudinal stretch is defined by the distance between the two particles in the deformed state divided by that in the undeformed state, $\lambda_1=dl/dR$. In terms of the functions $r(R)$ and $z(R)$, the longitudinal stretch is

$$\lambda_1 = \sqrt{\left(\frac{dr}{dR}\right)^2 + \left(\frac{dz}{dR}\right)^2} \,. \tag{1}$$

Consider the latitudinal stretch by examining a circle of material particles, of perimeter $2\pi R$ in the undeformed state. In the deformed state, the circle of particles occupy a circle of places, of perimeter $2\pi r(R)$. Thus, the latitudinal stretch is

$$\lambda_2 = \frac{r}{R} \,. \tag{2}$$

To characterize the kinematics of charging, we use nominal electric displacement; See Suo et al. (2008) and Dorfmann and Ogden (2005) for more general discussion. In the deformed state, let $\tilde{D}$ be the nominal electric displacement, namely, the electric charge on an element of an electrode in the deformed state divided by the area of the element in the undeformed state. Consequently, in the deformed state the total electric charge on the electrode is

$$Q = 2\pi \int \tilde{D} R dR \,. \tag{3}$$

Together, λ_1, λ_2 and $\tilde{D}$ are the three kinematic variables that characterize the state of an element of the membrane.

The membrane is a thermodynamic system, taken to be held at a constant temperature. Let W be the Helmholtz free energy of an element of the dielectric in the deformed state divided by the volume of the element in the undeformed state. Consequently, the Helmholtz free energy of the entire membrane in the deformed state is $2\pi H \int W R dR$. We stipulate that the free-energy density is a function of the three kinematic variables, $W(\lambda_1, \lambda_2, \tilde{D})$.

When the kinematic variables vary by small amounts, the free-energy density varies by

$$\delta W = s_1 \delta\lambda_1 + s_2 \delta\lambda_2 + \tilde{E}\delta\tilde{D} \,. \tag{4}$$

This equation defines the three partial differential coefficients

$$s_1 = \frac{\partial W\left(\lambda_1, \lambda_2, \tilde{D}\right)}{\partial \lambda_1}, \tag{5a}$$

$$s_2 = \frac{\partial W\left(\lambda_1, \lambda_2, \tilde{D}\right)}{\partial \lambda_2}, \tag{5b}$$

$$\tilde{E} = \frac{\partial W\left(\lambda_1, \lambda_2, \tilde{D}\right)}{\partial \tilde{D}}. \tag{5c}$$

These partial differential coefficients can be readily interpreted from (4): s_1 is the longitudinal nominal stress, s_2 the latitudinal nominal stresses, and $\tilde{E}$ the nominal electric field. Once a free-energy function $W\left(\lambda_1, \lambda_2, \tilde{D}\right)$ is prescribed for a given material, (5) constitutes the equations of state.

We now combine the kinematics and thermodynamics to derive the field equations that govern the state of equilibrium. This approach avoids introducing the nebulous notion of electric body force; see Suo et al. (2008) for further discussion. When the rigid disk moves by a small distance δu, the applied force does work $F\delta u$. When a small amount of charge δQ flows from one electrode to the other, the applied voltage does work $\Phi \delta Q$. In a state of equilibrium, thermodynamics dictates that, for arbitrary variation of the system, the change in the Helmholtz free energy of the membrane should equal the sum of the work done by the applied force and the applied voltage, namely,

$$2\pi H \int_A^B \delta W R dR = F\delta u + \Phi \delta Q. \tag{6}$$

Let the membrane be in a state of equilibrium characterized by $r(R)$, $z(R)$ and $\tilde{D}(R)$, and let the state undergo a small variation characterized by $\delta r(R)$, $\delta z(R)$ and $\delta\tilde{D}(R)$. From (1) we obtain the associated variation in the longitudinal stretch, $\delta\lambda_1 = \cos\theta \frac{d(\delta r)}{dR} - \sin\theta \frac{d(\delta z)}{dR}$. Using (4) and integrating by parts, we obtain that

$$\int_A^B \delta W R dR = \left(R s_1 \cos\theta \delta r - R s_1 \sin\theta \delta z\right)\Big|_A^B + \int_A^B \left[\left(-\frac{d\left(R s_1 \cos\theta\right)}{dR} + s_2\right)\delta r + \frac{d\left(R s_1 \sin\theta\right)}{dR}\delta z + R\tilde{E}\delta\tilde{D}\right] dR \tag{7}$$

Comparing (6) and (7), and recalling that $\delta r(R)$, $\delta z(R)$ and $\delta\tilde{D}(R)$ are independent variations, we obtain that

$$2\pi H R s_1 \sin\theta = F\,, \tag{8}$$

$$\frac{d\left(R s_1 \cos\theta\right)}{dR} = s_2\,, \tag{9}$$

$$H\tilde{E} = \Phi\,. \tag{10}$$

Equations (8) and (9) can also be obtained by balancing forces in the directions of *z* and *r*, respectively, as done in the literature (e.g., Tezduyar et al., 1987). Equation (10) recovers the definition of the nominal electric field.

3. Stability of a state of equilibrium

The electromechanical instability of Stark and Garton (1955) has been analyzed by using a method of thermodynamics (Zhao and Suo, 2007; Norris, 2008), where both the state of equilibrium and its perturbation are taken to be homogenous. We now extend the analysis to the stability of an inhomogeneous field of equilibrium against inhomogeneous field of perturbation.

The membrane is in a state of equilibrium subject to prescribed force *F* and prescribed voltage Φ. The Gibbs free energy of the system is

$$G = 2\pi H \int_A^B W R dR - Fu - \Phi Q\,. \tag{11}$$

As indicated before, the free-energy density is a function $W\left(\lambda_1, \lambda_2, \tilde{D}\right)$. When the three kinematic variables $\left(\lambda_1, \lambda_2, \tilde{D}\right)$ are expressed using (1)-(3), the free energy *G* is a functional of $r(R)$, $z(R)$, and $\tilde{D}(R)$, the three functions that characterize the state of the membrane. The state of

equilibrium is stable against any small perturbation in $r(R)$, $z(R)$, and $\tilde{D}(R)$ if and only if the functional G is a minimum.

Let the membrane be in a state characterized by the three functions, $r(R)$, $z(R)$, and $\tilde{D}(R)$, and let a neighboring state be characterized by $r(R)+\delta r(R)$, $z(R)+\delta z(R)$, and $\tilde{D}(R)+\delta\tilde{D}(R)$. The difference in the Gibbs free energy between the two states, $G(r+\delta r, z+\delta z, \tilde{D}+\delta\tilde{D})-G(r,z,\tilde{D})$, may be expanded in terms of the variations δr, δz, and $\delta\tilde{D}$. In deriving the equilibrium equations in the previous section, we have only expanded the variation of the Helmholtz free energy (4) to the terms linear in the variations of the kinematic variables. To examine the stability of the state of equilibrium, we need to include the variations quadratic in the kinematic variables.

In a state of equilibrium, the variation of G linear in δr, δz, and $\delta\tilde{D}$ vanishes, as expected from the derivation in the previous section. The variation of G quadratic in the kinematic variables is

$$\begin{aligned} &G(r+\delta r, z+\delta z, \tilde{D}+\delta\tilde{D})-G(r,z,\tilde{D})= \\ &2\pi H\int_A^B\left(\begin{array}{l}\frac{1}{2}\frac{\partial^2 W}{\partial\lambda_1^2}(\delta\lambda_1)^2+\frac{1}{2}\frac{\partial^2 W}{\partial\lambda_2^2}(\delta\lambda_2)^2+\frac{1}{2}\frac{\partial^2 W}{\partial\tilde{D}^2}(\delta\tilde{D})^2 \\ +\frac{\partial^2 W}{\partial\lambda_1\partial\lambda_2\tilde{D}^2}\delta\lambda_1\delta\lambda_2+\frac{\partial^2 W}{\partial\lambda_1\partial\tilde{D}}\delta\lambda_1\delta\tilde{D}+\frac{\partial^2 W}{\partial\lambda_2\partial\tilde{D}}\delta\lambda_2\delta\tilde{D}\end{array}\right)RdR \end{aligned} \tag{12}$$

Consequently, the state of equilibrium is stable against any arbitrary perturbation in the kinematic variables if and only if the above integral is positive-definite for any arbitrary perturbation. This condition of stability is equivalent to requiring that the Hessian

$$\mathbf{K}=\begin{bmatrix}\frac{\partial^2 W}{\partial\lambda_1^2} & \frac{\partial^2 W}{\partial\lambda_1\partial\lambda_2} & \frac{\partial^2 W}{\partial\lambda_1\partial\tilde{D}} \\ \frac{\partial^2 W}{\partial\lambda_1\partial\lambda_2} & \frac{\partial^2 W}{\partial\lambda_2^2} & \frac{\partial^2 W}{\partial\lambda_2\partial\tilde{D}} \\ \frac{\partial^2 W}{\partial\lambda_1\partial\tilde{D}} & \frac{\partial^2 W}{\partial\lambda_2\partial\tilde{D}} & \frac{\partial^2 W}{\partial\tilde{D}^2}\end{bmatrix} \tag{13}$$

be positive-definite for every material particle in the membrane in the state of equilibrium.

The Hessian is a symmetric matrix, and therefore has three real-valued eigenvalues. When a state of equilibrium is stable, all three eigenvalues should be positive. When the instability sets in, one or more eigenvalues vanish. Consequently, the critical condition for the electromechanical instability is

$$\det(\mathbf{K}) = 0 \tag{14}$$

for at least one material particle of the membrane.

4. Material model

To carry out numerical calculations, we need to prescribe an explicit form of the free-energy function $W(\lambda_1, \lambda_2, \tilde{D})$. Here we adopt a material model, called the ideal dielectric elastomer, where the dielectric behavior is liquid-like, unaffected by deformation (Zhao et al., 2007). Specifically, the true electric displacement is linear in the true electric field, and the permittivity is independent of deformation. This material model seems to describe some experimental data (Koford et al., 2003), but is inconsistent with other experimental data (Wissler and Mazza, 2007). Nevertheless, this model has been used almost exclusively in previous analyses of dielectric elastomers. For a model of nonideal dielectric elastomers, see McMeeking and Landis (2005) and Zhao and Suo (2008). In what follows we develop results for the ideal dielectric elastomer.

The elastomer is assumed to be incompressible, so that the stretch in the thickness direction of the membrane, λ_3, relates to the longitudinal and latitudinal stretches as $\lambda_3 = 1/(\lambda_1\lambda_2)$. The thickness of the membrane is H in the undeformed state, and is $\lambda_3 H = H/(\lambda_1\lambda_2)$ in the deformed state. By definition, the true electric field E is the voltage divided by the thickness of the membrane in the deformed state, so that $E = \lambda_1\lambda_2\Phi / H = \lambda_1\lambda_2\tilde{E}$. The true electric displacement D is defined as the charge in the deformed state divided by the area of the membrane in the deformed state, so that $D = \tilde{D}/(\lambda_1\lambda_2)$.

For the ideal dielectric elastomer, following Zhao et al. (2007), we assume that the free-energy density takes the form

$$W\left(\lambda_1,\lambda_2,\tilde{D}\right)=\frac{\mu}{2}\left(\lambda_1^2+\lambda_2^2+\lambda_1^{-2}\lambda_2^{-2}-3\right)+\frac{\tilde{D}^2}{2\varepsilon}\lambda_1^{-2}\lambda_2^{-2}. \tag{15}$$

The first term is the elastic energy, where μ is the small strain shear modulus. The second term is the dielectric energy, where ε is the permittivity. As seen in (15), the elastomer is taken to be a network of long and flexible polymers obeying the Gaussian statistics, so that the elastic behavior of the elastomer is neo-Hookean. For the ideal dielectric elastomer, the dielectric energy per unit volume is $D^2/2\varepsilon$, and the permittivity ε is a constant independent of deformation. In (15) the dielectric energy has been expressed in terms of the nominal electric displacement $\tilde{D}$, a variable required by the function $W\left(\lambda_1,\lambda_2,\tilde{D}\right)$.

Inserting (15) into (5), we obtain the equations of state:

$$s_1=\mu\left(\lambda_1-\lambda_1^{-3}\lambda_2^{-2}\right)-\frac{\tilde{D}^2}{\varepsilon}\lambda_1^{-3}\lambda_2^{-2}, \tag{16a}$$

$$s_2=\mu\left(\lambda_2-\lambda_2^{-3}\lambda_1^{-2}\right)-\frac{\tilde{D}^2}{\varepsilon}\lambda_2^{-3}\lambda_1^{-2}, \tag{16b}$$

$$\tilde{E}=\frac{\tilde{D}}{\varepsilon}\lambda_1^{-2}\lambda_2^{-2}. \tag{16c}$$

Recall that the true stresses σ_1 and σ_2 relate to the nominal stresses as $\sigma_1=\lambda_1 s_1$ and $\sigma_2=\lambda_2 s_2$. We rewrite (16) in terms of the true quantities:

$$\sigma_1=\mu\left(\lambda_1^2-\lambda_1^{-2}\lambda_2^{-2}\right)-\varepsilon E^2, \tag{17a}$$

$$\sigma_2=\mu\left(\lambda_2^2-\lambda_2^{-2}\lambda_1^{-2}\right)-\varepsilon E^2, \tag{17b}$$

$$D=\varepsilon E. \tag{17c}$$

These equations are readily interpreted. For example, the first term in (16a) is the contribution to the stress due to the change of entropy associated with the stretch of the polymer network, and the second term is the contribution to the stress due to the applied voltage. Equation (17) in

various forms has been used in previous analyses (e.g., Wissler and Maza, 2005a; Goulbourne et al., 2005).

The Hessian is obtained by inserting (15) into (13), so that (Zhao and Suo, 2007)

$$\mathbf{K}=\begin{bmatrix} \mu\left(1+3\lambda_1^{-4}\lambda_2^{-2}\right)+\dfrac{3\tilde{D}^2}{\varepsilon}\lambda_1^{-4}\lambda_2^{-2} & 2\mu\lambda_1^{-3}\lambda_2^{-3}+\dfrac{2\tilde{D}^2}{\varepsilon}\lambda_1^{-3}\lambda_2^{-3} & -\dfrac{2\tilde{D}}{\varepsilon}\lambda_1^{-3}\lambda_2^{-2} \\ 2\mu\lambda_1^{-3}\lambda_2^{-3}+\dfrac{2\tilde{D}^2}{\varepsilon}\lambda_1^{-3}\lambda_2^{-3} & \mu\left(1+3\lambda_2^{-4}\lambda_1^{-2}\right)+\dfrac{3\tilde{D}^2}{\varepsilon}\lambda_2^{-4}\lambda_1^{-2} & -\dfrac{2\tilde{D}}{\varepsilon}\lambda_2^{-3}\lambda_1^{-2} \\ -\dfrac{2\tilde{D}}{\varepsilon}\lambda_1^{-3}\lambda_2^{-2} & -\dfrac{2\tilde{D}}{\varepsilon}\lambda_2^{-3}\lambda_1^{-2} & \dfrac{1}{\varepsilon}\lambda_1^{-2}\lambda_2^{-2} \end{bmatrix} \qquad (18)$$

5. Numerical results and discussions

The theory presented above results in coupled nonlinear differential and algebraic equations, which we solve numerically; see Appendix for an outline of the method. This section describes results and discusses their implications. As discussed above, the membrane is a thermodynamic system of two generalized coordinates: the displacement u of the rigid disk, and the amount of charge Q on either electrode. The respective work-conjugate loading parameters are the applied force F and the applied voltage Φ. In presenting results, we normalize the four variables into dimensionless forms: u/a, $Q/\left(2\pi a^2\sqrt{\varepsilon\mu}\right)$, $F/\left(2\pi aH\mu\right)$ and $\Phi/\left(H\sqrt{\mu/\varepsilon}\right)$.

Unless otherwise stated, we fix the applied force to $F/\left(2\pi aH\mu\right)$ = 2, and vary the voltage applied. In designing a device using the configuration in Fig. 1, three dimensionless parameters can be varied: a/A, b/B and b/a. We first fix the three parameters to specific values, $a/A=b/B=1.2$ and $b/a=4$.

Fig. 2 plots the cross section of the deformed shapes of the membrane. As the voltage increases, the membrane expands its area and lowers the disk. Observe that the cross section of the membrane is curved due to the deformation in three dimensions.

Fig. 3 plots the distribution of the stretches λ_1 and λ_2 in the membrane. As expected, both stretches increase with the voltage. At a fixed voltage, the longitudinal stretch λ_1 is largest at the inner end of the membrane, and monotonically reduces to the smallest value at the outer end. The latitudinal stretch λ_2 is held at prescribed values at the two ends by the disk and the ring, and reaches maximum in the middle region of the membrane.

Fig. 4 plots the distribution of the true stresses in the membrane. To balance the applied force in the *z* direction, eq. (8), the longitudinal stress σ_1 is always tensile. The latitudinal stress σ_2, however, can become compressive when the applied voltage is large. This loss of tension may cause the membrane to buckle. Fig. 4 shows that the stresses are inhomogeneous in the membrane, and the loss of tension is expected to occur first at the inner end of the membrane.

Fig. 5 plots the distribution of the true electric field in the membrane. Recall that the applied voltage Φ is homogenous in the membrane. Consequently, the true electric field, $E = \Phi\lambda_1\lambda_2 / H$, scales with $\lambda_1\lambda_2$. As shown in Fig. 3, the two stretches reach maximum in different regions in the membrane. Fig 5 shows that *E* increases monotonically from the outer end of the membrane to the inner end. Assume that electrical breakdown occurs when the true electric field exceeds a critical value. Consequently, we expect that electrical breakdown occurs at the inner end of the membrane when the voltage is too high.

Fig. 6 plots the distribution of $\det(\mathbf{K})$ in the membrane. At a fixed applied voltage, $\det(\mathbf{K})$ is lowest at the inner end, and increases monotonically from the inner end to the outer end. The level of $\det(\mathbf{K})$ decreases as the applied voltage increases. For example, when $\Phi/\left(H\sqrt{\mu/\varepsilon}\right) = 0.3$, the value of $\det(\mathbf{K})$ becomes negative in a region near the inner end, indicating that the membrane will undergo electromechanical instability.

Fig. 7 plots the relation between the voltage and the displacement of the rigid disk. The range of the displacement corresponds to the range of actuation of the device. Fig. 8 plots the

relation between the voltage and the electric charge on either electrode. The area under this curve corresponds to the work done by the voltage.

Fig. 9 shows the plane whose axes are the two generalized coordinates, the displacement of the disk and the charge induced on either electrode. A point on the plane represents a state of the transducer, and a curve on the plane represents a path of an electromechanical process. Fig. 9 plots several paths of constant applied force and paths of constant applied voltage.

As mentioned previously, the transducer has three parameters of design: a/A, b/B and b/a. These parameters may be varied to modify the performance of the transducer. As a example, Fig. 10 plots the relations between the applied voltage and u/u_0 by varing a/A and b/B while retaining $b/a = 4$. Here u is the displacement of the disk when the membrane is subject to a voltage, and u_0 is the displacement of the disk when the membrane is subject to no voltage. At a fixed voltage, u/u_0 increases with a/A = b/B.

In addition to the cases where a/A = b/B, Fig. 10 also includes a case when $a/A = 1.1$ and $b/B = 1.8$. Fig.11 gives the distributions of the true electric field when $a/A = 1.1$ and $b/B = 1.8$. In this case the true electric field in the membrane is nearly uniform.

As seen above, the various fields in the membrane are inhomogeneous. Consequently, some regions of the membrane may be on the verge of failure, while other regions are still far below the capacity. This uneven distribution of the fields leads to an inefficient use of the material. However, once a particular device is selected, and criteria for failure are specified, one can make judicious choice of the parameters of design (e.g., a / A, b / B and b / a), such that the material is used efficiently and various modes of failure are averted. Such an exercise of design is beyond the scope of this paper, but the method developed here should play an important role.

6. Concluding remarks

To produce large deformation, a membrane is usually subject to an intense electric field, and is susceptible to various modes of failure. Because the field in the membrane is inhomogeneous, the membrane may fail at a single point of high field, while the rest of the membrane operates much below its full capacity. This paper illustrates these issues by analyzing a configuration used in a family of commercial devices. We combine the kinematics of axisymmetric deformation with the thermodynamics of electromechanical interaction, and obtain both the governing equations for the inhomogeneous state of equilibrium and the condition for the stability of such a state against inhomogeneous field of perturbation. Numerical results illustrate several potential modes of failure, including electrical breakdown, electromechanical instability, loss of tension, and rupture by stretch. The approach can be used to optimize the design of electromechanical transducers for specific applications.

Acknowledgements

This work is supported by the National Science Foundation through a project on Large Deformation and Instability in Soft Active Materials. The visit of THH to Harvard University is sponsored by the Ministry of Education, of the People's Republic of China. THH also acknowledges the support of the National Natural Science Foundation of China (10602021) and the Chinese Postdoctoral Science Foundation (20060400209). XHZ acknowledges the support of the Founder's Prize, through the American Academy of Mechanics, sponsored by the Robert M. and Mary Haythornthwaite Foundation.

References

Adkins, J. E., Rivlin, R. S., 1952. Large elastic deformations of isotropic materials. IX. The deformation of thin shells. Philosophical Transactions of the Royal Society of London. Series A, Mathematical and Physical Sciences 244, 505-531.

Bar-Cohen, Y., 2002. Electroactive polymers as artificial muscles: A review. Journal of Spacecraft and Rockets 39**,** 822-827.

Bonwit, N., Heim, J., Rosenthal, M., Duncheon, C., Beavers, A., 2006. Design of commercial applications of EPAM technology. Proceedings of the SPIE 6168, 39-48.

Carpi, F., Rossi, D. D., Kornbluh, R., Pelrine, R., Sommer-Larsen, P., 2008. Dielectric elastomers as electromechanical transducers: Fundamentals, materials, devices, models and applications of an emerging electroactive polymer technology. Elsevier, UK.

Dorfmann, A., Ogden, R. W. , 2005. Nonlinear electroelasticity. Acta Mechanica 174, 167-183.

Duncheon, C., 2008. Commercial actuators and issues. Chapter 29 in Carpi, F., Rossi, D. D., Kornbluh, R., Pelrine, R., Sommer-Larsen, P., 2008. Dielectric elastomers as electromechanical transducers: Fundamentals, materials, devices, models and applications of an emerging electroactive polymer technology. Elsevier, UK.

Goulbourne, N. C., Mockensturm, E. M., and Frecker, M., 2005. A Nonlinear Model for Dielectric Elastomer Membranes. ASME Journal of Applied Mechanics 72, 899-906.

Goulbourne, N. C., Mockensturm, E. M., and Frecker, M., 2007. Electro-elastomers: large deformation analysis of silicone membranes, Int. J. Solids Structures 44, 2609-2626.

Kofod, G., Sommer-Larsen, P., Kornbluh, R., Pelrine, R., 2003. Actuation response of polyacrylate dielectric elastomers. Journal of Intelligent Material Systems and Structures 14, 787-793.

Koford, G., Wirges, W., Paajanen, M, Bauer S., 2007. Energy minimization for self-organized structure formation and actuation. Appl. Phys. Lett. 90, 081916.

Liu, Y. M., Ren, K. L., Hofmann, H. F., and Zhang, Q. M., 2005. Investigation of electrostrictive polymers for energy harvesting. Ieee Transactions on Ultrasonics Ferroelectrics and Frequency Control 52**,** 2411-2417.

McMeeking, R.M., Landis, C.M., 2005. Electrostatic forces and stored energy for deformable dielectric materials. Journal of Applied Mechanics 72, 581-590.

Moscardo,M., Zhao X.H., Suo, Z.H., Lapusta, Y., 2008. On designing dielectric elastomer actuators. http://imechanica.org/node/3443.

Mockendturm, E.M., Goulbourne, N., 2006. Dynamic response of dielectric elastomers. Int. J. Non-Linear Mech. 41, 388-395.

Norris A. N., 2008. Comment on "Method to analyze electromechanical stability of dielectric elastomers". Applied Physics Letters 92, 026101.

Plante, J.S., Dubowsky,S., 2006. Large-scale failure modes of dielectric elastomer, International Journal of Solids and Structures 43, 7727–7751.

Pelrine, R., Kornbluh, R., Pei, Q. B., and Joseph, J., 2000. High-speed electrically actuated elastomers with strain greater than 100%. Science 287**,** 836-839.

Pelrine, R. E., Kornbluh, R. D., and Joseph, J. P., 1998. Electrostriction of polymer dielectrics with compliant electrodes as a means of actuation. Sensors and Actuators a-Physical 64**,** 77-85.

Stark, K.H., Garton, C.G., 1955. Electric strength of irradiated polythene. Nature 176, 1225-1226.

Suo, Z. G., Zhao, X. H., Greene,W. H., 2008. A nonlinear field theory of deformable dielectrics. Journal of the Mechanics and Physics of Solids 56,467-486.

Tezduyar,T.E., Wheeler, L.T., Graux, L., 1987. Finite deformation of a circular elastic membrane containing a concentric rigid inclusion. Int. J. Non-Linear .Mechanics. 22, 61-72.

Wingert, A., Lichter, M. D., and Dubowsky, S., 2006. On the design of large degree-of-freedom digital mechatronic devices based on bistable dielectric elastomer actuators. Ieee-Asme Transactions on Mechatronics 11**,** 448-456.

Wissler, M., Mazza, E., 2005a. Modeling and simulation of dielectric elastomer actuators. Smart

Mater. Struct. 14, 1396-1402 .
Wissler,M., Mazza,E., 2005b. Modeling of a pre-strained circular actuator made of dielectric elastomers. Sensors and Actuators A 120, 184-192.
Wissler, M., Mazza, E., 2007a. Mechanical behavior of an acrylic elastomer used in dielectric elastomer actuators, Sensors and Actuators A 134, 494-504.
Wissler, M., Mazza,E., 2007b. Electromechanical coupling in dielectric elastomer actuators. Sensors and Actuators A:Physical 138, 384-393.
Xia, J. Q., Ying, Y. R., and Foulger, S. H., 2005. Electric-field-induced rejection wavelength tuning of photonic bandgap composites. Advanced Materials 17**,** 2463.
Zhao, X.H., Hong,W., Suo, Z.G., 2007. Electromechanical coexistent states and hysteresis in dielectric elastomers. Physical Review B 76,134113.
Zhao, X.H., Suo, Z.G., 2007. Method to analyze electromechanical stability of dielectric elastomers. Applied Physics letters 91, 061921.
Zhao, X.H., Suo, Z.G., 2008. Electrostriction in elastic dielectrics undergoing large deformation. Submitted for publication. http://imechanica.org/node/3500.

Appendix: Coupled differential and algebraic equations

Rewrite (1) as

$$\frac{dr}{dR} = \lambda_1 \cos\theta . \tag{A1}$$

A combination of (8) and (9) gives

$$\frac{d\theta}{dR} = -\frac{s_2}{s_1 R}\sin\theta . \tag{A2}$$

The stresses in (A2) are expressed using (16a) and (16b), which in turn are expressed as functions of r, λ_1 and Φ by using (2), (10) and (16c). Rewrite the algebraic equation (8) as

$$\left[1-\left(\frac{\Phi r}{R}\right)^2\right]\lambda_1^4 - \frac{F}{R\sin\theta}\lambda_1^3 - \left(\frac{R}{r}\right)^2 = 0 . \tag{A3}$$

In writing (A3), we have normalized F and Φ.

Once the force F and the voltage Φ are prescribed, the ordinary differential equations (A1) and (A2), together with the algebraic equation (A3), govern the three functions $r(R)$, $\theta(R)$ and $\lambda_1(R)$, subject to the boundary conditions $r(A)=a$, $r(B)=b$. The boundary value problem is solved by using the shooting method. Once $r(R)$ are $\theta(R)$ are solved, the function $z(R)$ is determined by integrating $dz = -\tan\theta dr$, subject to the initial condition $z(B)=0$. We have checked our numerical results with those in Tezduyar et al. (1987) for the special case when the disk is moved by the applied force, in the absence of the voltage.

Figures

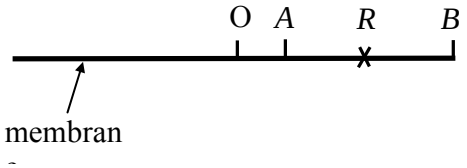

(a) Undeformed state

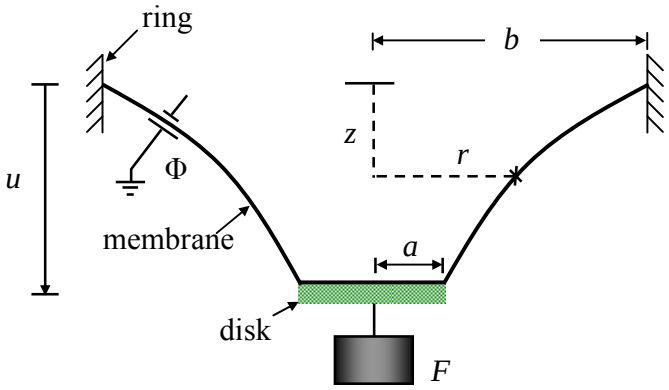

(b) Deformed state

Fig.1 Schematic cross section of an actuator. A circular membrane of a dielectric elastomer is sandwiched between two compliant electrodes. (a) In the undeformed state, the membrane is of radius *B*, and a particle of the membrane is at a distance *A* from the center O. Label a general particle of the membrane by the distance *R* of the particle from the center. (b) In the deformed state, the membrane is attached to a rigid circular disk of radius *a*, and to a rigid circular ring of radius *b*, such that the particle *A* moves to the place *a*, and the particle *B* moves to the place *b*. The ring is then held fixed, a force *F* is applied to the disk, and a voltage Φ is applied between the electrodes. In response to the applied load, the disk moves relative to the ring by a distance *u*, an amount of charge *Q* flows from one electrode to the other, and the particle *R* moves to a place with coordinates $r(R)$ and $z(R)$.

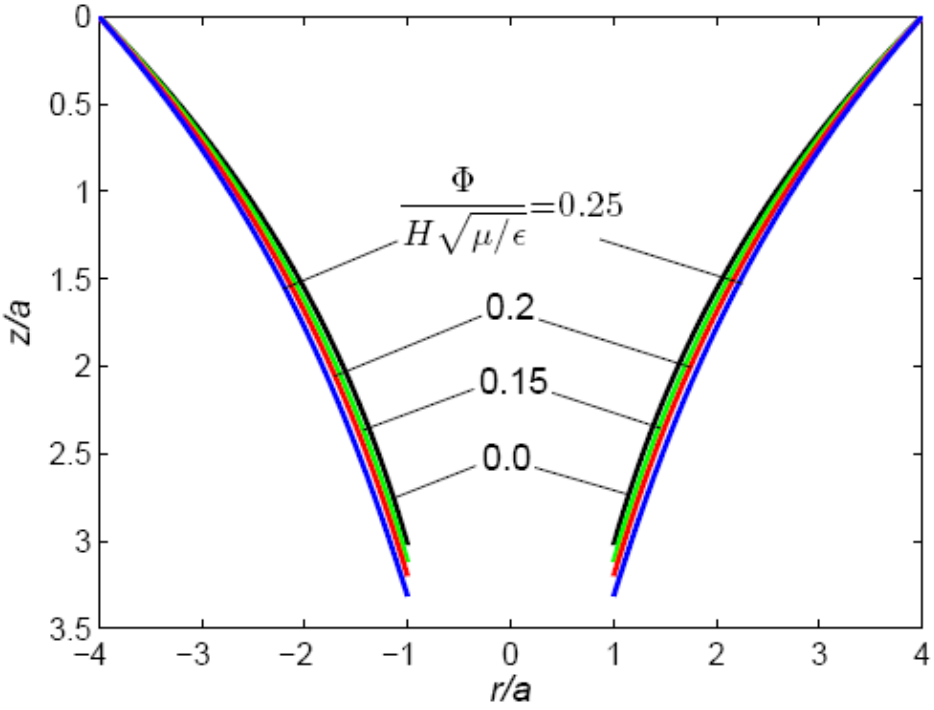

Fig.2 Deformed shapes of the membrane when the actuator is subject to a fixed force and several levels of voltage.

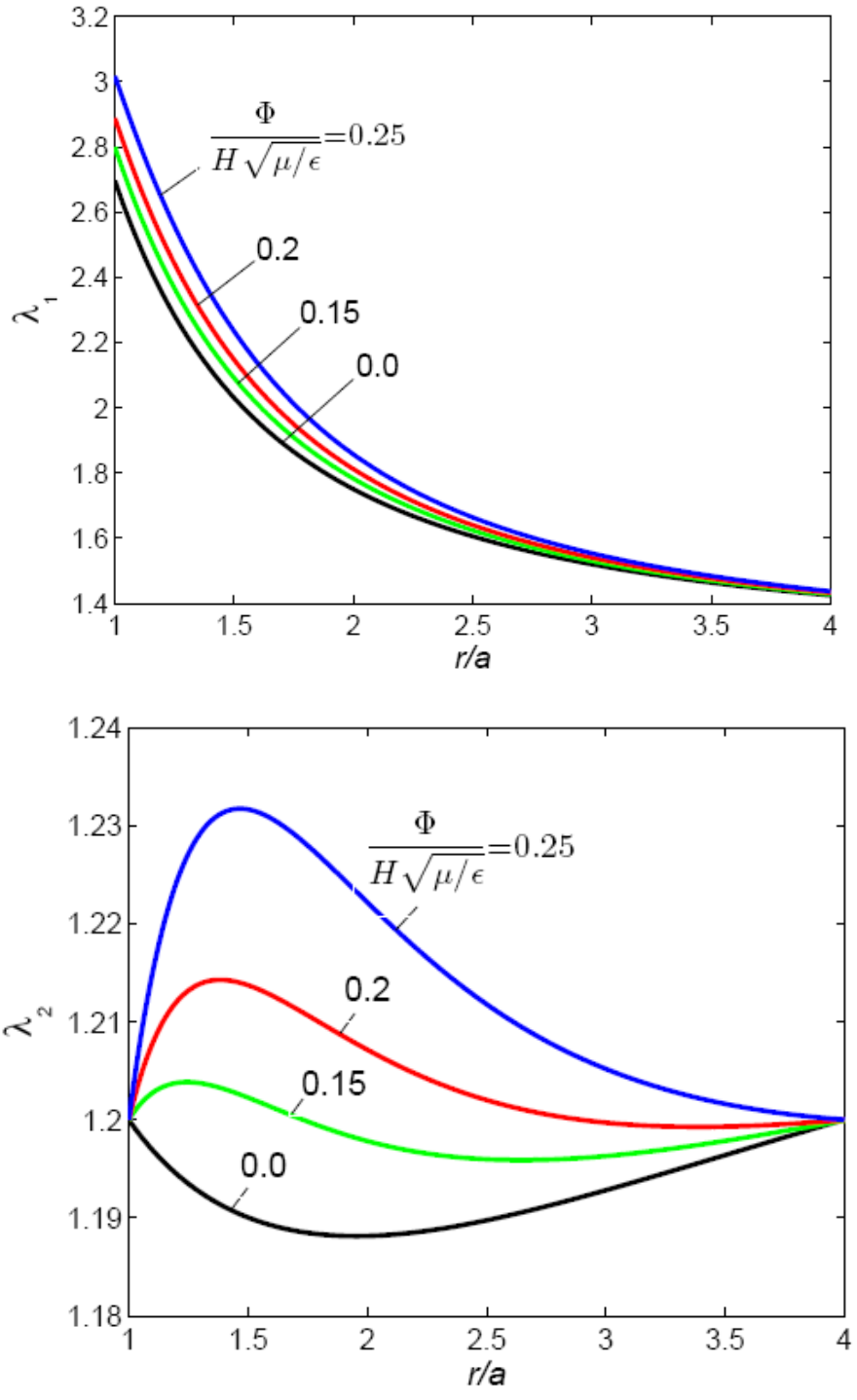

Fig.3 The distributions of stretches in the membrane.

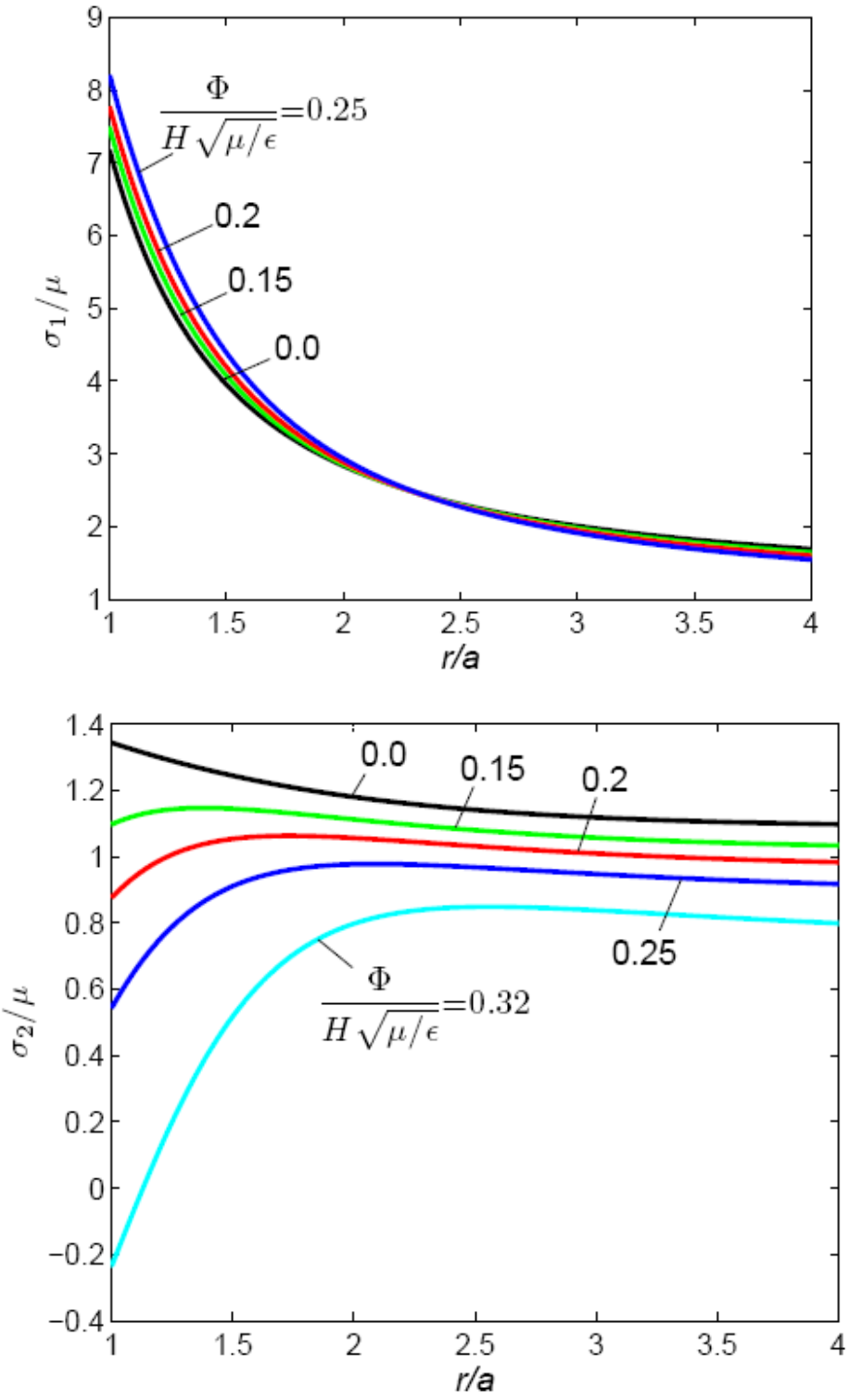

Fig.4 The distributions of true stresses in membrane.

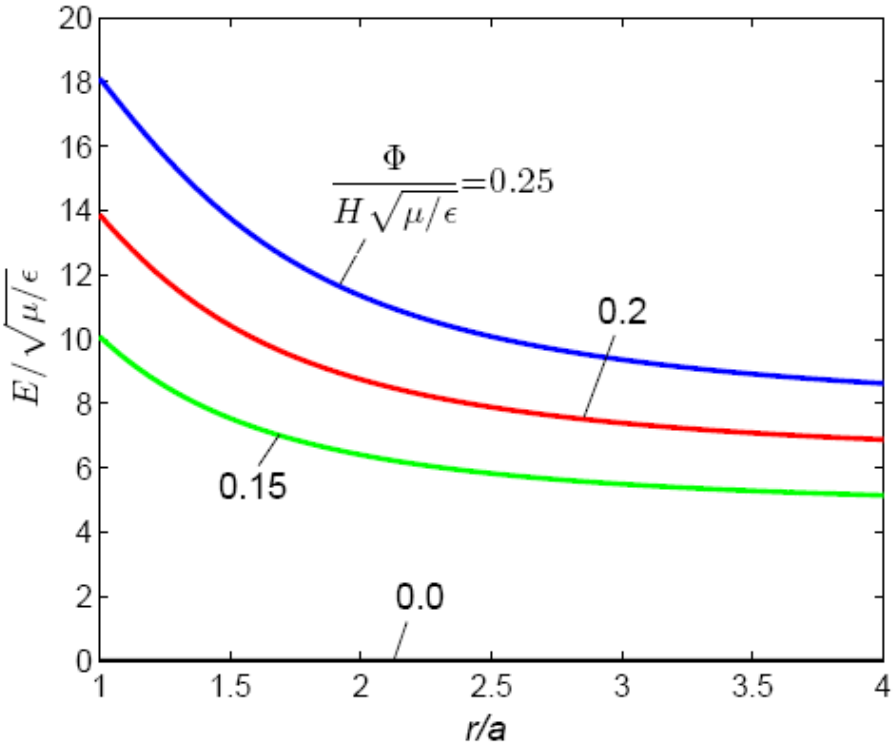

Fig.5 The distributions of true electric field in the membrane.

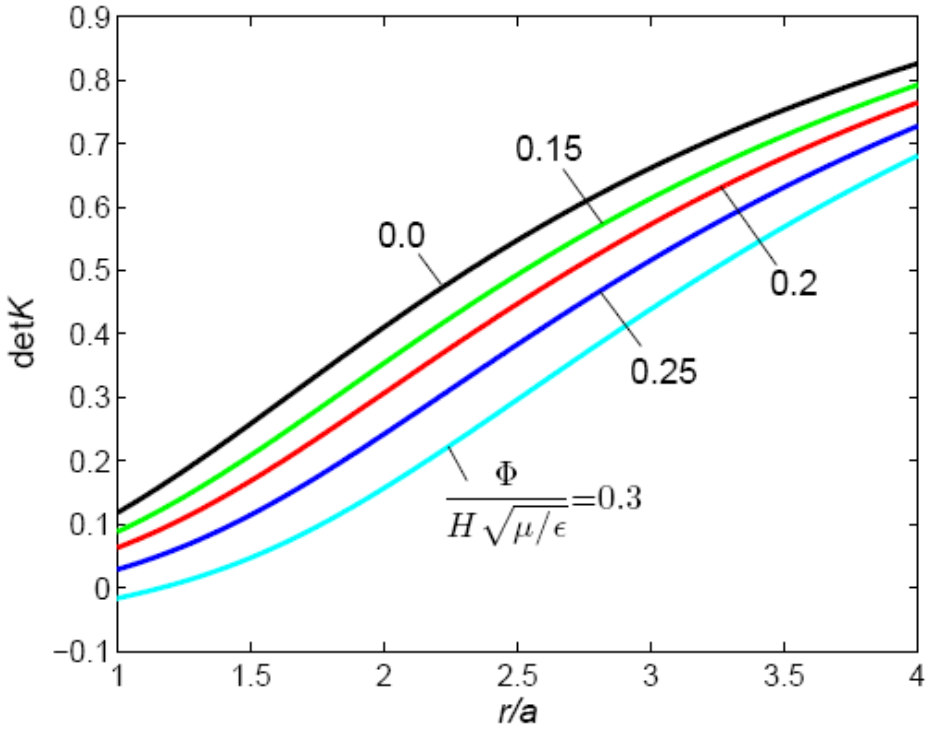

Fig. 6 The distributions of Hessian in the membrane

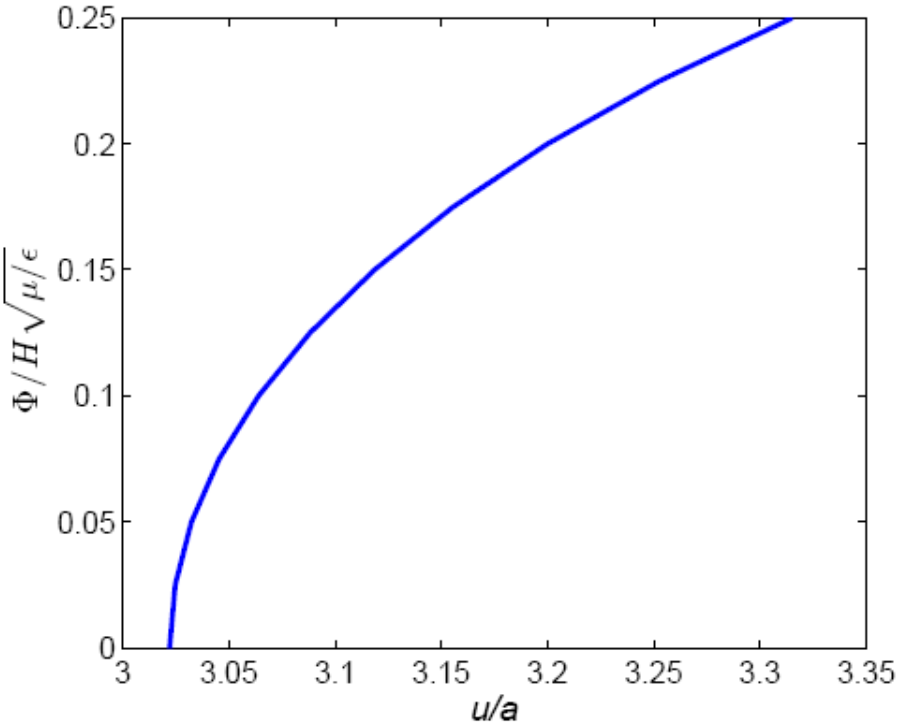

Fig.7 The relation between the applied voltage and the displacement of the disk.

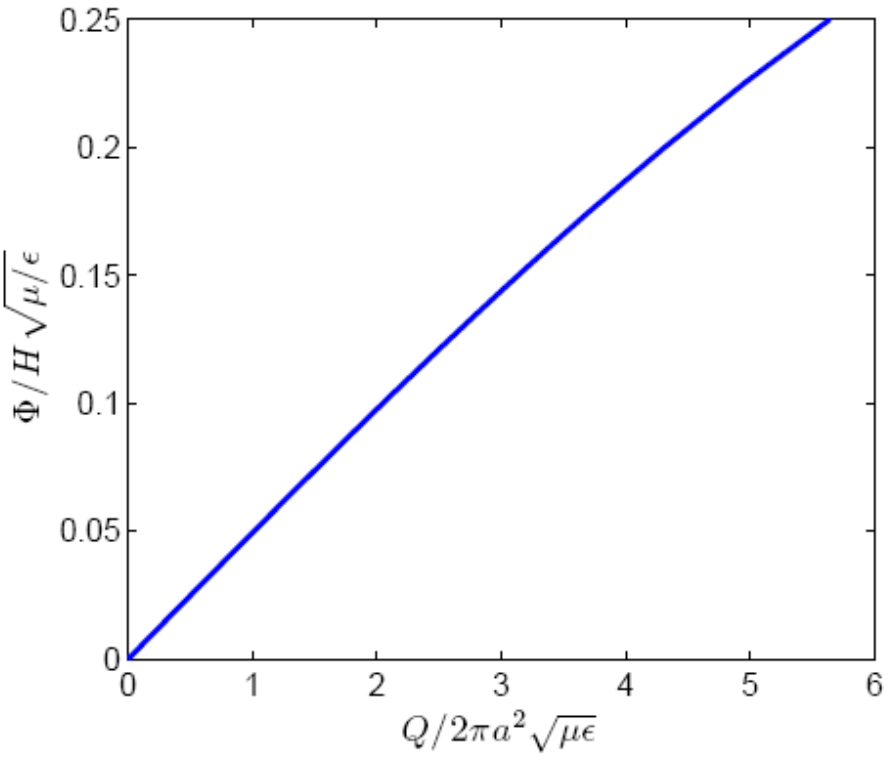

Fig.8 The relation between the applied voltage and the amount of electric charge on either electrode.

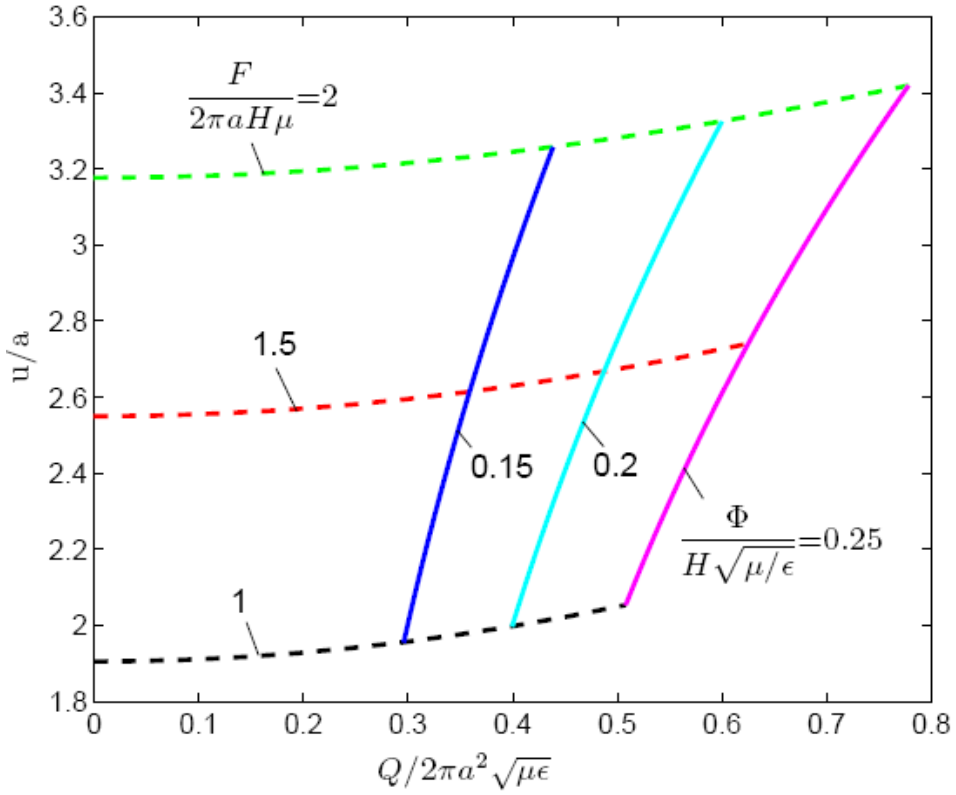

Fig.9 The actuator may be regarded as a thermodynamic system of two degrees of freedom, characterized by the generalized coordinates: the displacement of the disk, and the charge induced on either electrode. Their respective work-conjugate generalized forces are the mechanical force applied to the disk, and the electric voltage applied across the membrane. A point on the plane spanned by the two generalized coordinates represents a state of the actuator. A curve in the plane represents a path of actuation. Plotted in the plane are curves of constant applied force and curves of constant applied voltage.

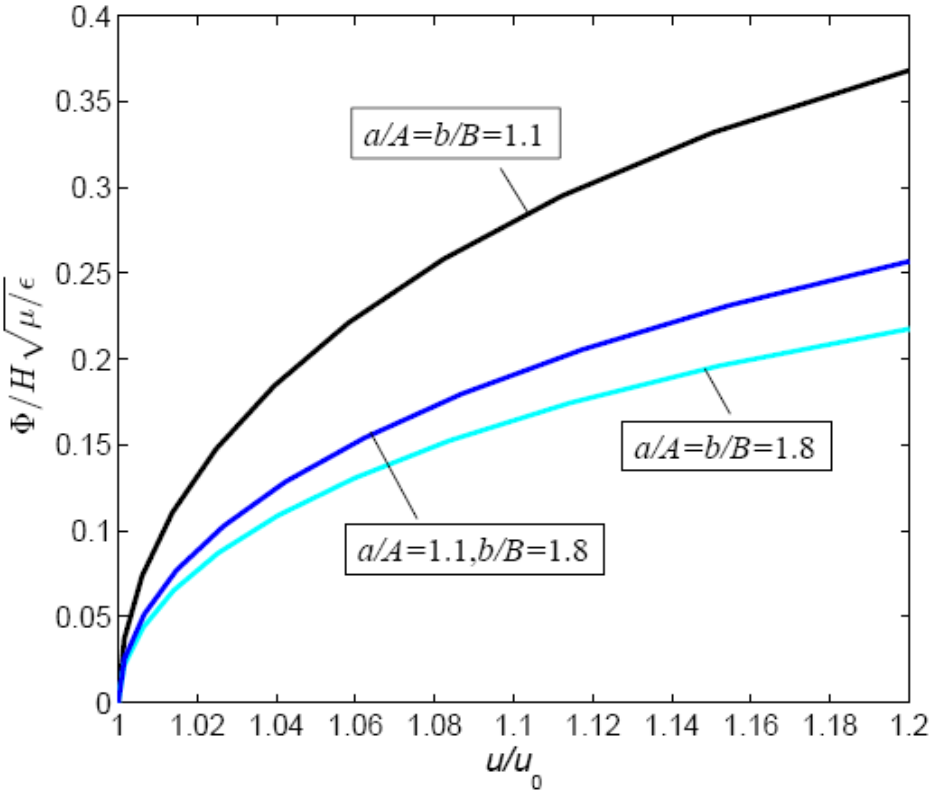

Fig.10 The relations of the applied voltages versus the ratio u/u_0 under several different a/A and b/B

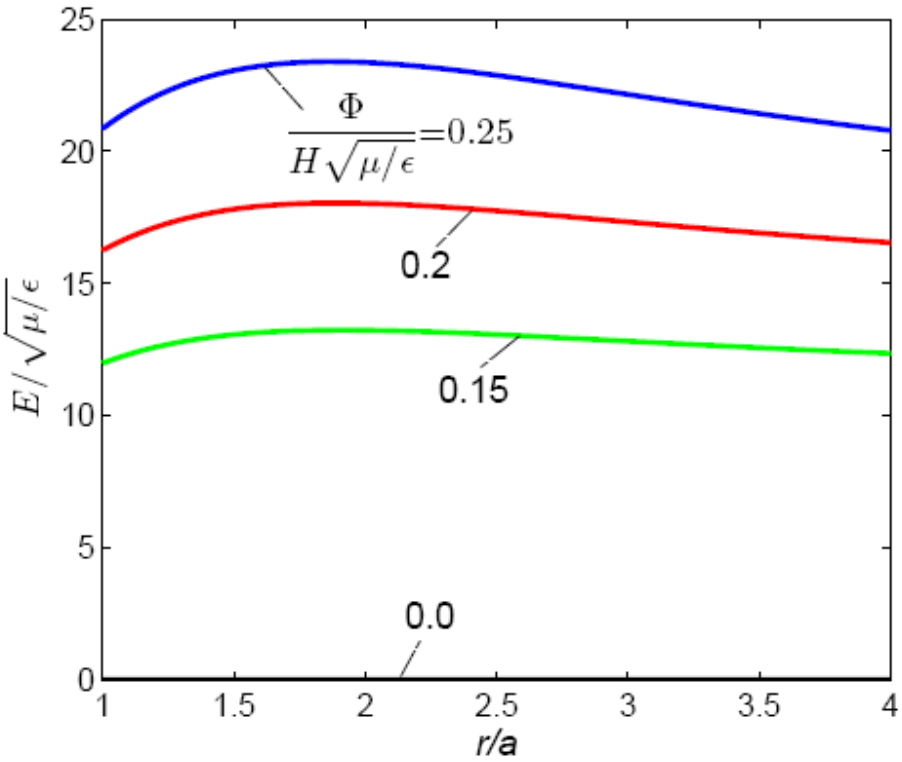

Fig.11 The distributions of true electric field in the membrane when $a/A=1.1$ and $b/B=1.8$